Int. J. Electrochem. Sci., 16 **(2021)** 150963, doi: 10.20964/2021.01.21

International Journal of
ELECTROCHEMICAL
SCIENCE
www.electrochemsci.org

Short Communication

Effect of Annealing on Microstructure and Capacitance Properties of Sol-gel TiO_2 Film on Aluminum

Huifeng Kang, Wenming Tian, Jialin Wu, Yiming Zhang, Zhonglei Li, Guoxing Pang,*

Heibei Key Laboratory of Trans-Media Aerial Underwater Vehicle, North China Institute of Aerospace Engineering, No.133 Aimindong Road, Langfang 065000, China.
*E-mail: tianwenming.dhr@163.com

Received: 9 September 2020 / *Accepted:* 20 October 2020 / *Published:* 30 November 2020

Sol-gel TiO_2 film prepared by dip-coating on aluminum was annealed under different temperatures, and subsequently anodized in ammonium adipate solution. The microstructure and capacitance properties of TiO_2 film on aluminum was investigated by X-ray diffraction (XRD), Raman spectroscopy (RS), thermogravimetric differential scanning calorimetry (TG-DSC), atomic force microscope (AFM), and capacitance temperature (C-T) test, respectively. The results indicated that TiO_2 film on aluminum annealed at 400 ºC and 500 ºC showed nanocrystalline anatase in 1-5nm and 5-12nm particles, respectively, while that annealed at 600 ºC showed mixed nanocrystalline phase (anatase and rutile) in 5-15nm particles. The anatase quantity developed remarkably with annealing temperature. The controlling factor of phase transformation of Sol-gel TiO_2 film was annealing temperature, and the aluminum foil substrate had little effect. Compared to specimens without TiO_2 film, the specific capacitance of TiO_2 coated specimens after anodizing at 400 ºC, 500 ºC and 600 ºC was increased by 15%, 35% and 74%, respectively.

Keywords: Aluminum electrolytic capacitor; anodizing; annealing; TiO_2 film;

1. INTRODUCTION

Aluminum electrolytic capacitors are extensively used in electric and electronic devices, such as notebook computer, mobile phone, and components in automobile industry, because of its outstanding characteristics of mini-bulk with large capacitance [1-6]. Now its capacitance can be further increased by incorporating high dielectric metal oxide into alumina and forming composite oxide [7,8]. Different composite oxide film prepared by different methods has been studied, such as Al-Si-O, Al-Zr-O, Al-Nb-O, and Al-Ti-O and so on [9-12].

TiO_2 exhibits excellent chemical and physical properties and characteristics, such as non-toxic, long term stability, good mechanical strength, transparency, and good insulating properties [13,14], and has been comprehensively researched and applied by now. TiO_2 has three main kinds of crystallographic

structures, namely brookite, anatase and rutile and their relative dielectric constant are about 30, 48 and 110-117, respectively [15,16]. Phase transformation process of these structures are mainly affected by annealing and preparation technology such as substrate, atmosphere et al [17,18].

Nanocrystalline dielectric thin film is usually observed by many methods, such as TEM, SEM and AFM. TEM has higher revolution, but electron beam would transform the original state of TiO_2 film, because high voltage electron beam would lead to re-crystallization. SEM could not distinguish original TiO_2 film without aided conductive materials, and the spraying conductive materials would cover the original surface of TiO_2. AFM is a method of in-situ and non-destructive investigation, which has high revolution and shows intuitionistic impression.

In some previous studies, an intermediate layer of Al-Ti-O nanocomposite film is confirmed to be formed between outer layer TiO_2 film and inner layer Al_2O_3 film during Sol-gel and anodizing process [19,20]. In this work, the effect of annealing on crystal type of TiO_2 film formed on aluminum was characterized by TG-DSC, XRD, Raman spectroscopy and AFM. The associated specific capacitance of the Al-Ti-O nanocomposite film prepared on aluminum was also discussed.

2. EXPERIMENTAL

2.1 Specimens preparation

TiO_2 Sol was firstly prepared by mixing tetrabutyl titanate, deionized water, acetyl acetone and dehydrated alcohol according to their molar ratio of 1:3:1:14, subsequently the mixture was stirred by magnetic force with 600 rpm/min for 30min and then aged at room temperature for about 48 h. Then, the electropolished aluminum foil (the aluminum purity is higher than 99.99%) with 50 μm thickness was immersed in TiO_2 Sol for 5 min and subsequently taken out with a withdrawing speed of 1 mm/S. The dip-coated aluminum foil was dried at 100 ºC in vacuum for 30min. And then the specimens were annealed at 400 ºC, 500 ºC, and 600 ºC for 10min in vacuum. When the annealing performed at different temperatures the heating rate was 50ºC/min. And then the dip-coated aluminum foil with TiO_2 film after annealing treatment was cut into 1×5 cm^2 specimens for the following tests. Finally, the specimens with and without TiO_2 film were all anodized at 50 V in ammonium adipate solutions (13wt%, pH≈6.9) at 85 ºC for 10 min by oxidation power equipment.

2.2 Characterization

Calorimetry measurement of dried Gel-Sol TiO_2 powder were performed by thermogravimetric differential scanning calorimetry (TG-DSC, Netzsh STA449C, Germany) at temperature range of 50 to 800 ºC with a heating rate of 20 ºC/min in the protective atmosphere of argon gas. The X-ray diffraction analysis (XRD, Rigakn D/max-2200, Japan) was also employed to characterized the crystal type of TiO_2 film which was stripped from coated specimens and of the dried Gel-Sol TiO_2 powder in a 2θ range of 20º to 90º at a step size of 0.02º using Cu K_α radiation. The Raman spectroscopy (Lab RAM HR800, JY Horiba, France) was also used to identify crystal phase of TiO_2 film annealed under different temperatures in an incident laser light at 633 nm wavelength and 4 × 4 μm^2 spot size. The surface

morphology of electropolished aluminum and TiO_2 film on aluminum annealed at different temperatures was observed by atomic force microscope (AFM, MutiMode Nanoscope, Veeco, USA) in tapping mode.

The values of specific capacitance for specimens were measured by multifrequency LCR meter (UC2852, Jiangsu Youce Electronic Ltd., China). The testing specimens were anodized aluminum foil with and without TiO_2 coating film and annealed at different temperatures. The specific capacitance was performed at volt potential of 3 V under constant current of 1mA and with a setting frequency of 120 Hz in 13 wt% ammonium adipate solution at room temperature. The LCR meter could directly figure out the specific capacitance values of different specimens during measurement.

3. RESULTS

3.1 Gel Powers structural properties

3.1.1 TG-DSC

Fig. 1 shows TG-DSC results of dried Gel TiO_2 powders in the temperature range from 50 ºC to 750 ºC. Residual water and some adsorbed alcohol molecular are gradually volatilized from 50 ºC to 250 ºC. An exothermic peak around 300 ºC indicates that the TiO_2 transforms from amorphous to brookite. And an exothermic peak between 400 ºC and 500ºC implies a process of amorphous transforming to anatase. A lot of mass loss occurs in a temperature range from 50 ºC to 500 ºC. While, there is little of mass loss beyond 500 ºC, which indicates that all of Gel TiO_2 powder totally transforms into anatase. The nearly flat curve after 500 ºC shows a slow process of anatase transforming to rutile. A tiny peak between 600 ºC and 700 ºC indicates that anatase begins to transform into rutile [19,20].

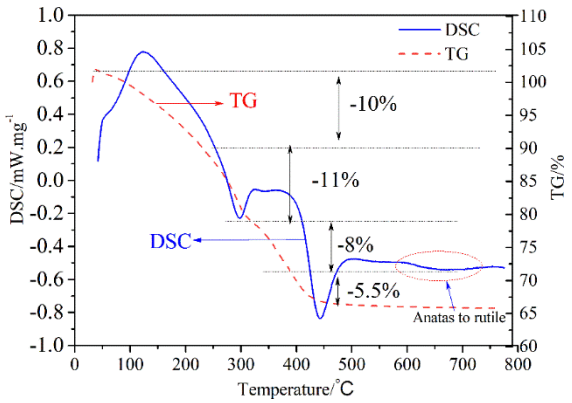

Figure 1. TG-DSC results of Gel TiO_2 powder

3.1.2 XRD

XRD results of dried Gel TiO_2 powder annealed at different temperatures are illustrated in Fig.2. There is only anatase phase in TiO_2 powder after annealing at 400 ºC and 500 ºC, and the TiO_2 powder annealed at 500 ºC has higher anatase intensity than that annealed at 400 ºC. The rutile characteristic

peak at about 2θ=27° is detected with weak intensity in 600 ºC annealed TiO_2 powder, which implies that a little content of rutile is formed. The rutile content in TiO_2 powder increases remarkably when annealing temperature increasing to 650 ºC. While, the TiO_2 powder annealed at 700 ºC completely transforms into rutile phase.

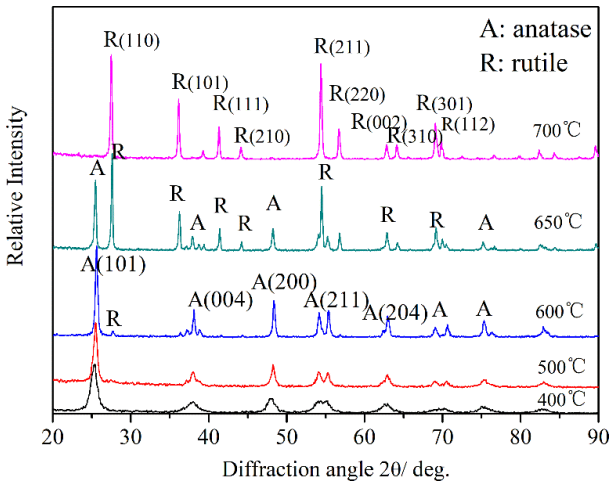

Figure 2. XRD patterns of TiO_2 powder annealed at different temperatures

The content of anatase and rutile phase in TiO_2 powder could be calculated by the following Formula (1) and (2), respectively [21]. Where, the X_A, X_B are the content proportion of anatase and rutile phase in crystalline TiO_2 powder, respectively. I_R and I_A denote the intensity of rutile phase and anatase phase in XRD pattern, respectively.

$$X_A(\%) = \frac{100}{1+1.265\frac{I_R}{I_A}} \qquad (1)$$

$$X_B(\%) = 1 - X_A \qquad (2)$$

The crystallization proportion in TiO_2 powder annealed at different temperatures is shown in Table 1. TiO_2 powder annealed at 600 ºC contains 91.7% anatase and 8.3% rutile; TiO_2 powder annealed at 600 ºC includes 63.5% anatase phase and 36.5% rutile phase.

Table 1. Transformation proportion of TiO_2 powder annealed at different temperatures

Annealing temperature/^{0}C	Anatase /%	Rutile/%
400 ℃	100%	0%
500 ℃	100%	0%
600 ℃	91.7%	8.3%
650 ℃	36.5%	63.5%
700 ℃	0%	100%

3.2 Structural properties of TiO_2 film on aluminum

3.2.1 XRD

TiO_2 film stripped from coated specimens was analyzed by XRD, which is displayed in Fig. 3. It shows that there is only anatase in TiO_2 film after 400 ºC annealing. And at 500 ºC, the intensity of anatase in TiO_2 increases remarkably compared to that annealed at 400 ºC. At 600 ºC, more anatase and a quantity of rutile are formed. The anatase phase intensity in XRD pattern increases remarkably with increasing annealing temperature. The other peaks are suggested to be $Al(OH)_3$ X-ray diffraction pattern, which are supposed to be coated on TiO_2 particles when metal aluminum was dissolved in NaOH aquatic solution. $Al(OH)_3$ reflections in XRD could be worked as an internal standard for intensity comparison between anatase and rutile annealed at different temperatures. According to Formula (2), the content of rutile phase in TiO_2 film annealed at 600 ºC is about 30%. The peak at $2\theta=25°$ for TiO_2 film annealed at 600 ºC is much sharper than that annealed at 500 ºC. According to Scherrer equation, it could be confirmed that the crystalline size of anatase grain in TiO_2 film becomes much bigger as temperature increased from 500 ºC to 600 ºC.

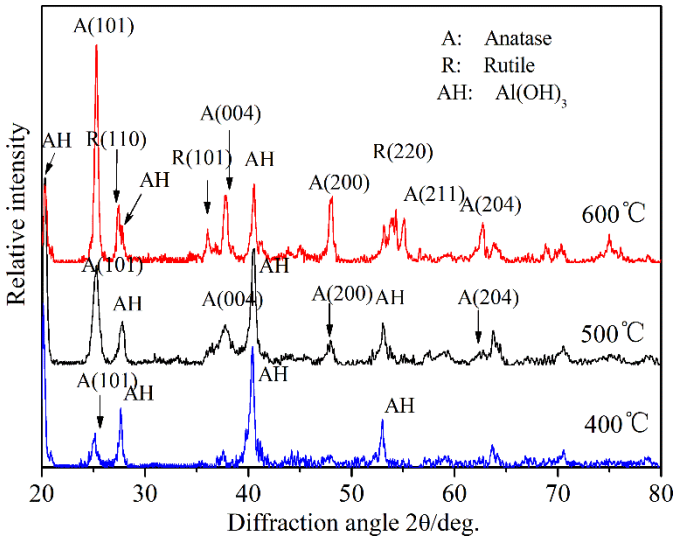

Figure 3. XRD patterns of TiO_2 film on aluminum foil annealed at different temperatures

3.2.2 Raman spectroscopy

Raman spectroscopy of TiO_2 film annealed at different temperatures is shown in Fig.4. Five well-defined peaks at 146cm^{-1}, 141cm^{-1}, 396cm^{-1}, 518cm^{-1} and 638cm^{-1} are supposed to be characteristic peaks of anatase. Peaks at 144cm^{-1}, 448cm^{-1} and 614cm^{-1} are defined as characteristic ones of rutile in Fig.4 [22,23]. It indicates that there is only anatase in TiO_2 film on aluminum when the annealing temperature being 400 ºC and 500 ºC. By contrast, both the anatase and a spot of rutile exists in TiO_2 film on aluminum when the annealing temperature being 600 ºC. The intensity of characteristic peak around 144cm^{-1} of TiO_2 film annealed at 500 ºC is two as big as the 400 ºC annealed one. Anatase phase intensity of TiO_2 film annealed at 600 ºC keeps increasing compared to the 500 ºC annealed film. It

indicates that the anatase content increases greatly with increasing annealing temperature. At 600 ºC, the intensity of rutile phase is remarkable, about 30% of anatase.

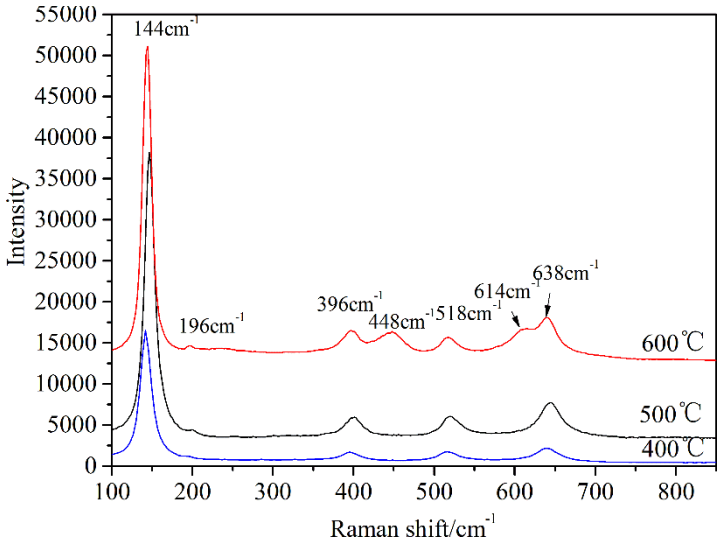

Figure 4. Raman spectroscopy of TiO_2 film formed on aluminum annealed at different temperatures

3.2.3 AFM morphologies

The surface morphologies of specimens before and after annealing at different temperatures were observed by AFM, as shown in Fig. 5. According to Fig.5 (a, b), the electropolished aluminum has the lowest roughness, which means that aluminum has extremely smooth surface. Gel TiO_2 film is very dense, and composed of fine particles about 2-4 nm (Figs.5c, d). The size of TiO_2 particles on the annealed film increases with increasing annealing temperature. The TiO_2 particle size on film annealed at 400 ºC is about 5-7nm; its value is about 5-12 nm at 500 ºC annealing, and increases to about 5-15 nm as annealing temperature increased to 600 ºC. As shown in AFM 3D and 2D images of Fig.5 (e-j), The average particles size and roughness of TiO_2 film annealed at different temperatures are listed in Table 2.

Table 2. Average grain size and roughness of TiO_2 film annealed at different temperatures

Annealing temperature/ ℃	Average grain size/nm	Roughness/nm
400 ºC	7.086	0.398
500 ºC	13.036	0.768
600 ºC	15.102	1.163

The TiO_2 film becomes denser and more compact with temperature increasing. AFM morphology of TiO_2 film annealed at 400 ºC is similar with that of Gel film. It indicates that crystal quantity in film

annealed at 400 ºC is smaller than that annealed at 500 ºC and 600 ºC. The AFM result is in close agreement with the measurements of Raman spectroscopy and XRD test.

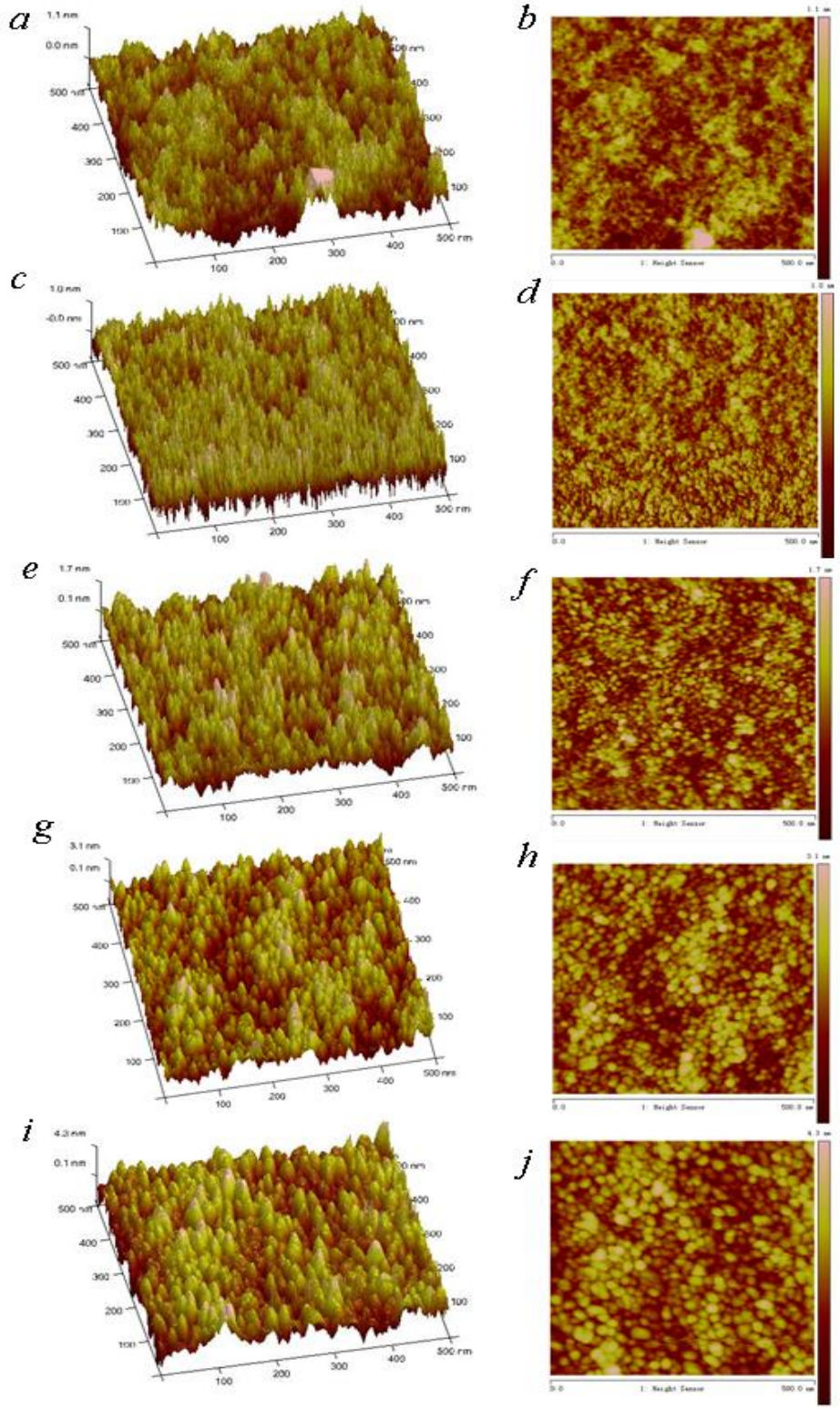

Figure 5. AFM surface morphology in 2D and 3D of electropolished aluminum (*a, b*), and TiO_2 on aluminum before (*c, d*), and after annealing at 400℃ (*e, f*), 500℃ (*g, h*), and 600℃ (*i, j*)

3.3 Capacitance-Temperature tests

The specific capacitance of coated specimens annealed at different temperatures is shown in Fig. 6. Compared to the specimens without TiO_2 film, the specific capacitance of coated specimens is improved about 15.6%, 38.3% and 74% after 400 ºC, 500 ºC and 600 ºC annealing, respectively. It indicates that the specific capacitance of coated specimens increases remarkably with increasing annealing temperature. It shows that the dielectric constant of Al-Ti-O composite film prepared by sol-gel and anodizing increases with more crystal phase content in TiO_2 film.

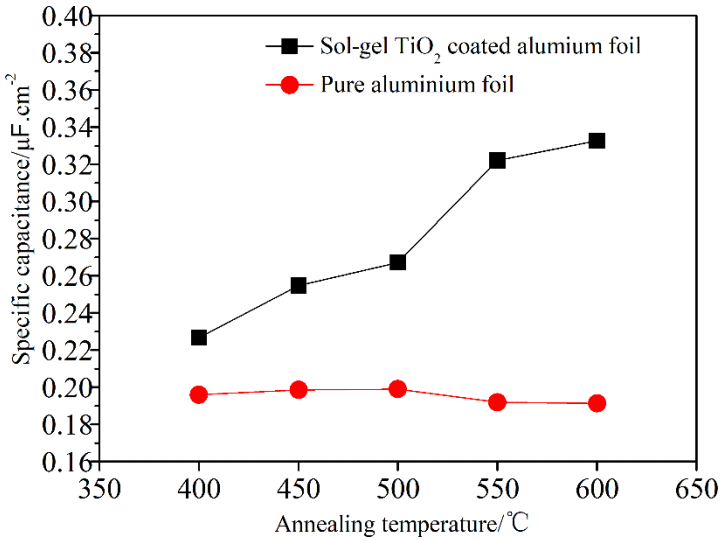

Figure 6. Specific capacitance of specimens with and without TiO_2 film annealed at different temperatures

4. DISCUSSION

4.1 Structural properties

As mentioned above, the TiO_2 powder and TiO_2 film had similar phase transformation during annealing in the temperature range from 400 ºC to 600 ºC. Crystal state in TiO_2 powder was nearly consistent with the TiO_2 film at different annealing temperature. But at 600 ºC, the content of rutile in TiO_2 film was 20% higher than that in TiO_2 power. It indicated that aluminum substrate had little effect on phase transformation of TiO_2 film, and the annealing temperature was a main effect on transformation of crystal phase for TiO_2 film.

Amorphous TiO_2 began to transform into anatase with minor amount at temperature range of 400 to 500 ºC. TiO_2 film on aluminum consisted of massive anatase and a small number of rutile in about 30% when annealing temperature being 600 ºC. The quantity of anatase increased remarkably with increasing annealing temperature. Anatase would entirely transform into rutile at 700 ºC. TiO_2 film on aluminum annealed at different temperatures was composed of nano-particles. Higher temperatures promoted the nucleation and growth of crystals, and thus the size of TiO_2 particles increased with

annealing temperature.

4.2 Dielectric properties

The TiO_2 film was homogeneously coated on the wall surface of the etched aluminum foils, and thus the holes were covered by TiO_2 film, which decreased the real area of etched aluminum foils. Besides, the coated TiO_2 film increased the total thickness of specimens. Therefore, the specific capacitance of aluminum foil should decrease theoretically after TiO_2 film coating according to the equation (3), where ε_0 is the vacuum permittivity, ε_r is the relative permittivity of the anodic oxide film, S is effective surface area of the dielectric oxide film, d denotes the thickness of the oxide film.

$$C = \frac{\varepsilon_0 \varepsilon_r S}{d} \qquad (3)$$

However, the real area and real thickness of specimens were mainly determined by the anodic oxide layer formed after anodizing. The anodic oxide layer is highly multihole and far thicker than the pure aluminum foil and TiO_2 film, and its specific surface area is also far bigger than the original surface area of etched aluminum foil. Therefore, the original thickness of aluminum foil and TiO_2 film as well as the surface area of etched foil had relatively light effect on the specific capacitance of specimens. The specific capacitance of specimens was mainly determined by the crystal texture of the composite film.

For the porous structure of TiO_2 film, the improvement of specific capacitance of specimens was owed to the Al-Ti-O nanocomposite film. The Al-Ti-O composite film is suggested to be a compact composite structure which is composed of TiO_2 particles and anodic alumina [20]. With annealing temperature increasing from 400 ^oC to 600 ^oC, TiO_2 film on aluminum becomes denser and more compact, as well as with more anatase and rutile. As a result, Al-Ti-O composite film contains more anatase or rutile phase after a higher temperature annealing. Therefore, dielectric constant of the composite Al-Ti-O film increases greatly with increasing annealing temperature. In consequence, specific capacitance of specimens coated with TiO_2 film is improved remarkably.

Mitra [24] used mechanical milling to introduce different strain-leaves to the multiphase TiO_2 powder. A longer time mechanical milling resulted in a more significant strain induced partial phase transformation to the rutile phase and more oxygen vacancies. These phases changes could increase about 30% to about 60% capacitive performance compared to the commercial TiO_2 powder. Besides, Mitra found that the powder size had little effect on the capacitive properties. While, Ashery [25] believed that the effect of TiO_2 phase changes on capacitive properties was still limited. He designed a composite GO/TiO_2/n-Si MOS device, and obtained a specific capacitance up to about 5.0×10^{-7} F/cm^2, which was 60% to 100% higher than our work, however with a more complicated preparation process. Raj [26] pointed out that the increased specific surface area could remarkably increase the areal capacitance of the TiO_2 electrode. He prepared a TiO_2 nanotube arrays electrode with a very high carrier density and a huge specific area, which resulted in a highest areal capacitance of 20.09 mF/cm^2 to this TiO^2 electrode. Zhang [27] developed a manufacturing process to produce a TiO_2 nanotube arrays/C/MnO_2 composite electrode and obtained an amazing specific areal capacitance of 492 mF/cm^2, which was the highest value can be found in literatures in present. Compared to these above studies, it

can be found that the improvement of specific capacitance caused by TiO_2 phase transformation is limited but with the most simplified preparation process. The composite TiO_2 nanotube arrays electrode embellished by metallic oxides always showed a far better specific areal capacitance but with a very complex manufacturing process, which would obviously increase the cost. Which preparation route being the best depends on the cost performance.

5. CONCLUSIONS

(1) In summary, annealing temperature is a controlling factor on phase transformation of TiO_2 film formed on aluminum, and the substrate has little effect on phase transformation. In TiO_2 film on aluminum, there were only anatase phase after 400 ºC and 500 ºC annealing. Both rutile and anatase phases formed in TiO_2 film during 600 ºC annealing, and the rutile phase accounted for 30% in hybrid crystal phases. Anatase phase in TiO_2 film increased remarkably with temperature increasing.

(2) The specific capacitance of coated specimens after anodizing increased with annealing temperature. Compared to the pure aluminum foil, the specific capacitance of specimens with TiO_2 film annealed at 400 ºC, 500 ºC and 600 ºC increased by 15%, 35% and 74%, respectively.

ACKNOWLEDGEMENTS
This research is sponsored by the Local Science and Technology Development Funds Founded by Central Government under Grant No. 206Z1902G, Key Projects of the State Administration of Science, Technology and Industry for National Defense under Grant No. JCKY2018407C006, Youth Fund of the Hebei Natural Science Fund project under Grant No. E2019409052, and the Education Department Science Research project of Hebei under Grant No. QN2019104.

References

1. S. Park, and B. Lee, *J. Electroceram.*, 13 (2004) 111.
2. K. Watanabe, M. Sakairi, H. Takahashi, K. Takahiro, S. Nagata, and S. Hirai, *J. Electrochem. Soc.*, 148 (2001) B473.
3. W. Tian, F. Chen, Z. Li, G. Pang, and Y. Meng, *Corros. Sci.*, 173 (2020) 108775.
4. W. Tian, F. Chen, Z. Li, G. Pang, and Y. Li, *Int. J. Electrochem. Sci.*, 15 (2020) 6572.
5. W. Tian, F. Chen, F. Cheng, Z. Li, and G. Pang, *Int. J. Electrochem. Sci.*, 15 (2020) 9120.
6. W. Tian, Z. Li, H. Kang, F. Cheng, F. Chen and G. Pang, *Materials*, 13 (2020) 3236.
7. H.G. Redda, R.S. Chen, and W.N. Su, *Int. J. Electrochem. Sci.*, 14 (2019) 7758.
8. Z. Feng, J. Chen, R. Zhang, and N. Zhao, *Ceram. Int.*, 38 (2012) 3057.
9. Q.Y. Wang, S. Liu, Y.R. Tang, R. Pei, Y.C. Xi, and D.X. Zhang, *Int. J. Electrochem. Sci.*, 14 (2019) 3740.
10. J. Chen, Z. Feng, and B. Yang, *J. Mater. Sci.*, 41 (2006) 569.
11. Z.S. Feng, J.J. Chen, C. Zhang, N. Zhao, and Z. Liang, *Ceram. Int.*, 39 (2012) 2501.
12. J. Chen, Z. Feng, M. Jiang, and B. Yang, *J. Electroanal. Chem.*, 509 (2006) 26.
13. J. Shi, Q. Qian, H. Jiang, H. Li, S. Wang, F. Wei, and D. Feng, *Int. J. Electrochem. Sci.*, 15 (2020) 845.
14. J. Luo, X. Yu, S. Li, and R. Diao, *Int. J. Electrochem. Sci.*, 14 (2019) 8206.
15. Y. Abe, and T. Fukuda, *Jan J. Appl. Phys.*, 33 (1994) L1248.

16. H. Shin, M.R. De Guire, and A.H. Heuer, *J. Appl. Phys.*, 83 (1998) 3311.
17. P. Lobl, M. Huppertz, and D. Mergel, *Thin solid films*, 251 (1994) 72.
18. S.S. Lin, *Ceram. Int.*, 38 (2012) 2461.
19. L. Yao, J. Liu, M. Yu, S. Li and H. Wu, *T. Nonferr. Metal. Soc.*, 20 (2010) 825.
20. J. Liu, Q. Guo, M. Yu, and L. Yao, *ECS J. Solid State Sci. and Technol.*, 2 (2013) N55.
21. J. Liu, R. Yang, and S. Li, *J. Rare Earths*, 25 (2007) 173.
22. I.A. Alhomoudi, and G. Newaz, *Thin solid films*, 517 (2009) 4372.
23. A. Orendorz, A. Brodyanski, J. Lösch, L.H. Bai, Z.H. Chen, Y.K. Le, C. Ziegler, and H. Gnaser, *Surf. Sci.*, 600 (2006) 4347.
24. D. Mitra, S. Bhattacharjee, N. Mazumder, B.K. Das, P. Chattopadhyay, and K.K. Chattopadhyay, *Ceram. Int.*, 46 (2020) 20437.
25. A. Ashery, H. Shaban, S.A. Gad, and B.A. Mansour, *Mat. Sci. Semicon. Proc*., 114 (2020) 105070.
26. C.C. Raj, V. Srimurugan, A. Flamina, and R. Prasanth, *Mater. C. Phys.*, 248 (2020) 122925.
27. Z. Zhang, Z. Xu, Z. Yao, Y. Meng, Q. Xia, D. Li, and Z. Jiang, *J. Alloy.Compd.*, 805 (2019) 396.